Journal of Metals, Materials and Minerals, 33(4), 1732, 2023

Synthesis and modification of nickel hydroxide particle synthesized by self-assembly and electron beam irradiation technique for photocatalyst activity

Narisara SAECHIN[1,†], Sumitra SRIPHO[1,†], Thitirat RATTANAWONGWIBOON[2,*], Sakchai LAKSEE[2], Pattra LERTSARAWUT[2], Wilasinee KINGKAM[2], and Sarute UMMARTYOTIN[1,3,*]

[1] *Department of Materials and Textile Technology, Faculty of Science and Technology, Thammasat University, Pathumthani, 12120, Thailand*
[2] *Thailand Institute of Nuclear Technology, Ongkharak, Nakorn Nayok, 26120, Thailand*
[3] *Center of Excellence on Petrochemical and Materials Technology, Chulalongkorn University, Bangkok, 10330, Thailand*

***Corresponding author e-mail:** sarute@tu.ac.th; thitirat@tint.or.th
† These authors contributed equally to this work.

Received date:
7 May 2023
Revised date
8 August 2023
Accepted date:
9 August 2023

Keywords:
Electron beam irradiation;
Nickel hydroxide;
Self-assembly;
Photocatalyst

Abstract

The purpose of this work is to study the methyl orange removal of $Ni(OH)_2$ nanoparticles. The photocatalyst activity is investigated based on UV lamp of 18 watt. $Ni(OH)_2$ is synthesized by a self-assembly process and then exposed to electron beam radiation at 10 MeV energy with various doses ranging from 50 kGy to 500 kGy. The properties of $Ni(OH)_2$ nanoparticles are then evaluated. No significant change of functional group and percent of crystallinity are observed. The morphology is uniformly presented as a plate-like. The specific surface area, pore size and pore volume are reduced. Point of zero charge confirmed that positive charge is presented onto the surface. It therefore provides strong affinity to negative charge of dye removal. As-synthesized $Ni(OH)_2$ particle exhibits the excellent properties for methyl orange adsorption and photocatalyst activity over methyl orange degradation. It was remarkable to note that $Ni(OH)_2$ particle is therefore considered as an excellent candidate for dye degradation in textile industry.

1. Introduction

With the rapid increase of worldwide population, the push towards to development of semiconductor-based material has been extensively evident. The application of semiconductor prepared from nano-sized particle illustrates various applications due to unique optical properties. It typically involves numerous sectors of research such as UV photolithography, light emitting diode, dye synthesized solar cell as well as photocatalyst. Among many optical usages, one of the most attractive applications is typically referred to photocatalyst-based material. It is defined as an acceleration of a photoreaction in the existence of photocatalyst. It can be interacted at the excited state in order to form the reaction intermediate and to regenerate into a small molecule. With the presence of photocatalyst, it can be generated into free radicals after UV- and visible light activation. It can be therefore enrolled in many sectors of application such as wastewater remediation, self-cleaning glass as well as antibacterial activity.

Up to the present time, various metal based particles are successfully synthesized for photocatalyst. One of the most effective particles is focused on nickel hydroxide particle. It is defined as a chemical compound with an empirical formula of $Ni(OH)_2$. The use of $Ni(OH)_2$ particle significantly provides numerous advantages including an electrolyte in nickel plating solution, oxygen donor in auto emission catalyst and anodizing aluminum process in glass frit for porcelain enamel and/or cermet. Recently, Liao *et al*. [1] evaluated the presence of nickel based particle in enamel for self-healing behavior at elevated temperature of oxidation process. It can improve the flexural strength and thermal shock resistance. The nickel particle deflected crack phenomena at the interface. Li *et al*. [2] found that the existence of nickel particle can increase the thermal stability and oxidation resistance of $La_{3-x}Te_4$ compound. The oxidation rate was significantly decreased in both air and low oxygen partial pressure. It is notable that with the nickel based particle, it offers the great perspective for excellent dimensionless thermoelectric. Moreover, Fatimah *et al*. [3] investigated the role of nickel based particle for photocatalyst. It can be used to modify the surface of reduced graphene oxide. It is considered as an excellent candidate for photocatalytic activity for oxidation of tetracycline. It also offers the excellent antibacterial activity with low minimum inhibitory concentration. Kuo *et al*. [4] synthesized $Ni(OH)_2$ based composite for energy storage device. It offered high electrochemical properties as well as excellent efficiency of supercapacitor. Zhao *et al*. [5] also successfully synthesized $Ni(OH)_2$ based compound for supercapacitor. It exhibited hierarchical structure with fast electron/ion transport. It can be therefore employed as an electrode.

In order to synthesize $Ni(OH)_2$ particle with additional perspective of controllable properties, various synthetic routes have been extensively investigated. It is remarkably noted that reliable, rapid and accurate of product should be considered as top priority of synthesis. In recent year, Dhas *et al*. [6] studied the nickel based particle synthesized by sol-gel formation route. This technique allows us to prepare nickel based particle with uniform morphology. However, the impurities are still presented. It subsequently results in less performance of application. Karol *et al*. [7] studied the process of solid state reaction for metal oxide particle formation. Although it can form metal oxide with controllable properties, the processing is limited due to high temperature usage. It may provide the difficulty for large scale of production. Durai *et al*. [8] evaluated the hydrothermal process for metal oxide synthesis. It is still limited due to reactor design. In order to overcome these issues, novel synthetic procedure based on thermo-dynamic equilibrium at ambient temperature is purposed. Self-assembly technique is considered as one of the most effective strategies in order to synthesize metal oxide particle. This technique significantly provides numerous benefits including uniformity and high percent yield product. Noppakuadrittidej *et al.* [9] used this technique to synthesize silica bead. The uniformity in size and shape of product are obtained. It offers the great promise for optical properties in colorimetric sensor in food spoilage determination. Phutanon *et al*. [10] synthesized CuO flower-like architecture by self-assembly technique. With the variation of pH range, it can be synthesized into uniform size and shape. It also offers the excellent performance of photocatalytic activity.

Apart from synthetic route, nickel-based compound is successfully prepared. One of the most important applications is focused on photocatalyst. Aejitha *et al*. [11] studied the La-doped into nickel based particle for photocatalyst. The study involved DFT calculations and degradation mechanism. Moradi *et al*. [12] synthesized nickel based compound as a nano-photocatalyst. It can be employed to remove the pharmaceutical pollutant. To date, in order to enhance the photocatalyst activity, surface modification of metal oxide particle is considered as one of the most important targets. With wide range of specific surface area and porosity, it may provide the benefit as heterogeneous catalyst. It is typically referred to an active site for catalytic reaction as suggested by Ahmad *et al.* [13]. One way to improve the surface properties is typically related to electron beam irradiation technique. It involves to use electron at high energy to treat an object for a variety of purpose, as indicated by Li *et al.* [14]. Sokovnin *et al.* [15] used this technique to modify the magnetic, thermal and luminescent properties of metal oxide particle. This technique reflects the transformation of defect in metal oxide particle. Kugai *et al.* [16] reported that electron beam irradiation technique can be used to synthesize metal oxide particle. It can be prepared from aqueous phase under mild condition.

With significant enhancement of surface properties of metal oxide modified by electron beam irradiation, photocatalyst activity for dye degradation is therefore considered as an important target. With the exponential growth of textile industry, dye removal and wastewater treatment are typically involved. Photocatalyst activity provides the great promise for remediation. It can be responded to eco-friendly and sustainable purpose. Therefore, the objective of this work is to prepare nickel hydroxide particle by self-assembly technique. Surface modification by electron beam irradiation is employed. Physico-chemical properties are then examined. After that, preliminary test for dye remediation is also reported.

2. Experimental

2.1 Chemical reagents

Nickel nitrate hexahydrate ($Ni(NO_3)_2$ $6H_2O$) with 99% of purity is purchased from KemAus, Co, Ltd. The molecular weight is 290 $g{\cdot}mol^{-1}$. The boiling point and density are 136°C and 2.05 $g{\cdot}mL^{-1}$, respectively. Reagent grade of 35% purity of ammonia (NH_3) and methyl orange are purchased from Sigma Aldrich, Co, Ltd. The molecular weight of ammonia is 35 $g{\cdot}mol^{-1}$. The boiling point and density are 37.7°C and 0.88 $g{\cdot}mL^{-1}$, respectively. They are employed as a solvent and dye molecule, respectively. All of chemical reagents are used as received without any further purification.

2.2 Methodology

2.2.1 Synthesis of nickel hydroxide particle by self-assembly technique

2 M of nickel hydroxide particle is successfully synthesized by self-assembly technique based on the guidance of Phutanon *et al.* [17] with modification. Briefly, 3 g of nickel nitrated hexahydrate is dissolved into 5 mL of deionized water. It is continuously stirred at room temperature for 30 min in order to ensure the complete solubility. Then, small amount of ammonia is dropped into a solution. The pH of solution is set to the range of 6 to 12 by ammonia solution. It is stirred for 1 h until complete nucleation process. Then, solvent is removed by suction flask which connected to vacuum pump. The powder is washed several times with water and ethanol. It is dried at 50°C for 4 h. It is stored in desiccator in order to avoid the moisture absorption.

2.2.2 Surface modification of nickel hydroxide particle by electron beam irradiation technique

The as-synthesized powder is undergone electron beam irradiation technique. The electron beam chamber is set to 10 MeV. The energy is controlled to be 50 kGy to 500 kGy. It is conducted for 3 h. To avoid the moisture absorbent, the as-modified powder should be kept in desiccator.

2.2.3 Application of nickel hydroxide particle as a photocatalyst

To investigate the properties of nickel hydroxide particle as a photocatalyst, the degradation behavior of methyl orange is observed under an external applied UV. The UV lamp of 18 watt is purchased from Philips, Co., Ltd. The initial concentration of methyl orange in DI water is set to be 2×10^{-5} M. It is poured into 15 mL in beaker. The pH of 7 is prepared for methyl orange concentration. 15 mg of nickel hydroxide particle is poured into the solution. The mixture is continuously stirred for 1 h in order to ensure the saturation of methyl orange absorption onto the surface. After that, it is stored in Eppendorf

and continuously centrifuged for 30 min. Then, the remained solution is investigated by UV-visible spectroscopy in the wavelength of 300 nm to 600 nm. For the photocatalyst experiment, the centrifugation is conducted for 1 h under an external applied UV. The time is recorded within 5 h. Then, the absorbance is calculated with a maximum wavelength of 465 nm. The percent removal is therefore determined based on Equation (1)

$$\% \text{ Removal} = (A_0\text{-}A_t)/A_0 \times 100\% \quad (1)$$

where A_0 is referred to initial absorbent and A_t is referred to absorbent at investigation time, respectively.

2.3 Instrument

2.3.1 Field emission scanning electron microscopy

The nickel hydroxide powder is investigated using SEM (SEM, Quanta 250 microscope, Japan). The specimens are gold-coated using a sputtering device (JEOL, JFC-1200) prior to the SEM observation. A magnification and accelerating voltage of 30 kX and 2 kV are used.

2.3.2 Fourier transform infrared spectroscopy

The nickel hydroxide powder is investigated using FTIR. The spectra are recorded using a Nicolet iS50 Thermo Scientific, USA. KBr is used as the reflection element. DTGS ATR is used as the detector. The range of wavenumber of 4000 cm^{-1} to 400 cm^{-1} is employed. The resolution of ±4 cm^{-1} and a number of scans of 64 are set.

2.3.3 X-ray diffraction

The crystal structure of nickel hydroxide powder is investigated by X-ray diffraction (XRD, Phillips P.W. 1830 diffractometer). It employs nickel filtered CuKa radiation. Diffraction patterns are recorded over a range of 20° to 80°. Prior to the investigation, the sample is stored in a desiccator to prevent moisture absorption.

The percent of crystallinity is calculated based upon integration method where straight background line compares to the area under entire curve with area under the crystalline peak.

% of crystallinity = (area under the crystalline peaks/area under all peaks) × 100

The crystal size is calculated based on Scherrer equation, where $L = K\lambda /(\beta \cos\theta)$. Briefly, K is referred to Scherrer constant, θ is referred to diffraction angle, λ is referred to wavelength and β is referred to full width at half maximum.

2.3.4 BET analysis

The specific surface area, pore size and pore volume of nickel hydroxide powder are reported by BET analysis. This technique permits to analyze based on the guidance of Adsorption analyzers Flex 6.01, Micromeritics Instrument, USA. It is typically related to multipoint gas adsorption. Before N_2 adsorption analysis, the sample is degassed at 300°C for 2 h. The Brunauer-Emmett-Teller (BET) technique is used to evaluate.

2.3.5 Dynamic light scattering

This technique is used to analyze the size of nickel hydroxide particle. It is used based on the guidance of Zetasizer, refractive index of 1.43 absorption 0.001. The sample is poured into DI water. The concentration is set to be 0.1 $mg{\cdot}mL^{-1}$. The mixture is stirred for 30 min and subsequently sonicated for 30 min in order to ensure the uniformity.

2.3.6 UV-Vis spectroscopy

This technique is employed to determine the concentration of methyl orange solution. With the presence of nickel hydroxide powder as a catalyst, the concentration of methyl orange solution is subsequently reduced with respect to the increment of investigation time. The measurement is conducted by UV-VIS spectrophotometer under the wavelength region of 300 nm to 600 nm.

2.3.7 Point of zero charge (PZC) analysis

This technique allows us to investigate the electric charge onto nickel hydroxide particle. Briefly, 10 mL of 0.1 M of KCl is used to adjust pH by adding 0.1 M of NaOH and 0.1 M of HCl. The pH is set to be 4, 6, 8, 10 and 12, respectively. The solution is continuously stirred for 15 min. Then, 10 mg of as-synthesized $Ni(OH)_2$ powder is poured into the mixture. It is continuously stirred at room temperature for 3 days in order to ensure the uniformity. Then, point of zero charge is reported with respect to pH. The data is presented based on statistical average

3. Results and discussion

Nickel hydroxide is successfully synthesized by self-assembly technique. It is presented as a greenish-color in fine powder form. With the variation of pH range during synthetic procedure, the percent yield of product is different based on the presence of [OH] concentration. It can be induced to form the nickel hydroxide particle by nucleation and growth as suggested by Kim *et al.* [18]. The existence of hydroxide group may be considered as a reducing agent. It is then introduced to reduce Ni^{2+} ion into nickel hydroxide particle. It is observed that as soon as nickel precursor is decreased, the colloidal particle of nickel hydroxide is therefore occurred. It is uniformly distributed into suspension. This is in agreement with previous literature of Musino *et al.* [19]. Furthermore, it is notable that the presence of hydroxide group can attach onto the surface of nickel oxide particle leading to controllable size and shape uniformity. It may form the electrostatic force between Ni^{2+} ion and hydroxide group [20]. It can promote the complexation of Ni^{2+} and also form the passivation contact for nickel oxide stabilization as suggested by Raveendran *et al.* [21]. On the other hand, with the existence of hydroxide group, it may lead to improve the dispersion state. This negative charge can increase the accessibility of the nucleation site.

Figure 1 reports the XRD pattern of $Ni(OH)_2$ as a precursor source synthesized by self-assembly route. The electron beam irradiation technique is employed to modify surface. With the variation of energy, no significant change of peak is observed. All of patterns are presented in the similar characteristic peaks. However, it is observed that with increment of electron beam irradiation ray, the intensity of peak is relatively high. It may consequently result in increment of percent of crystallinity, as suggested by Meid *et al.* [22]. In this analysis, it can be confirmed that single phase of $Ni(OH)_2$ as a precursor source is successfully synthesized. Six sharp peaks are observed at the 2θ of 19°, 33°, 37°, 52°, 58° and 63°. These peaks are corresponded to diffraction plane of [001], [100], [011], [012], [110] and [111] respectively. The crystal structure and space group are hexagonal and P3m1, No.164, respectively. It is confirmed according to the standard pattern of JCPDS No. 38-0715. These peaks are similar to previous article reported by Wang *et al.* [23]. It can be explained that $Ni(OH)_2$ is considered as a set of disordered structure, but not yet to a well-defined polymorph [24]. Furthermore, it is observed that without electron beam irradiation technique, low crystallinity is therefore observed. It may probably consider based upon large interlayer space of $Ni(OH)_2$ phase. It may intrinsically intercalate by hydroxyl group. It consequently results in the expansion of interlayer space, as indicated by Delmas *et al.* [25]. With the increment of electron beam irradiation technique, the absence of water molecule may disappear, leading to significant increase of peak's intensity. It may therefore result in superiority of percent crystallinity.

Table 1 reports the percent of crystallinity and crystal size of $Ni(OH)_2$ as a precursor source modified by electron beam irradiation technique. The percent of crystallinity and crystal size are approximately reported to be 82% to 87% and 5 nm to 7 nm, respectively. It is notable that under the electron beam irradiation technique, no significant change is observed. This technique is only employed to modify the surface of $Ni(OH)_2$ as a precursor.

Moreover, in order to modify the surface properties of as-synthesized nickel oxide particle, the variation of electron beam irradiation is employed. Figure 2 reports the FTIR spectra of nickel hydroxide synthesized by self-assembly technique with variation of electron beam irradiation. It is important to note that during self-assembly synthesis, the formation of nickel hydroxide as a precursor source is obtained. It may form nickel oxide particle later on. However, in order to compare as a control sample, nickel hydroxide as a precursor source is provided. All of characteristic peaks are typically presented in the similar feature. It is observed that no change of functional group is observed. This is probably due to the fact that electron beam irradiation uses low energy of absorption onto sample surface [26]. It is observed that the characteristic peak at 3600 cm^{-1} is presented. This broad peak is attributed to OH stretching. The hydroxyl group is presented due to the adherence of water molecule onto surface of nickel oxide powder. It can be used to guide that to store this sample in desiccator should be preferable, as suggested by Akhtar *et al.* [27].

In order to determine the morphological properties of as-synthesized $Ni(OH)_2$ as a precursor source, scanning electron microscope is then employed. The microstructure is typically presented as a plate form. The size and shape are uniformly presented based on its thermodynamic equilibrium [28]. The orientation of plate form is well ordered into "flower-like" feature. It is therefore self-assembled from a single plate composed by oriented attachment of nano-flower, as suggested by Li *et al.* [29]. It is observed that with the electron beam irradiation stage, no significant change of size and shape is thus observed. It provides the effect onto surface of precursor.

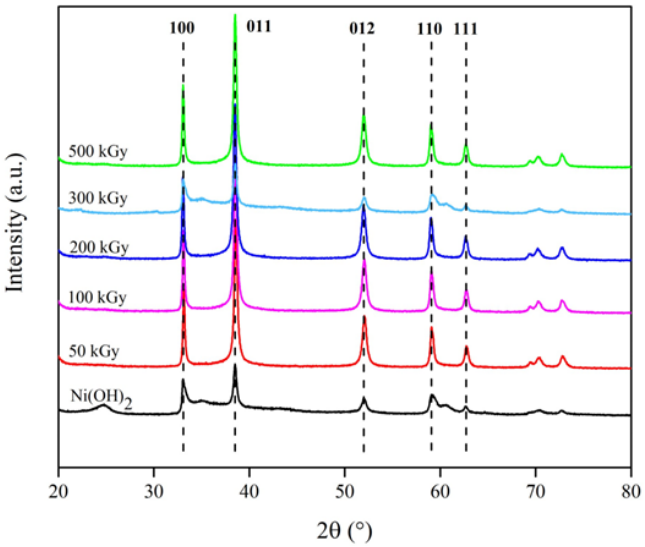

Figure 1. XRD pattern of $Ni(OH)_2$ as a precursor source modified by electron beam irradiation technique.

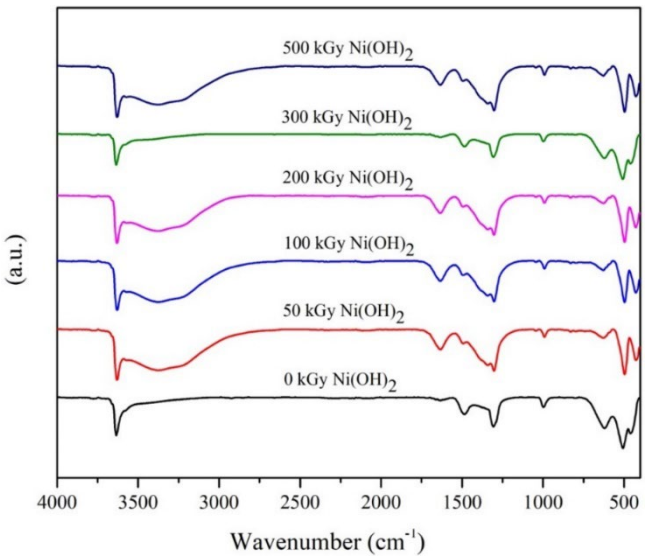

Figure 2. FTIR spectra of $Ni(OH)_2$ as a precursor source modified by electron beam irradiation technique.

Table 1. Percent of crystallinity and crystal size of $Ni(OH)_2$ as a precursor source modified by electron beam irradiation technique.

Sample	%Crystallinity	Crystal size (nm)
0 kGy	86.5647	5.8224
50 kGy	83.7890	6.8229
100 kGy	84.1898	6.7660
200 kGy	82.8566	6.3632
300 kGy	85.5513	6.3107
500 kGy	83.9637	5.9672

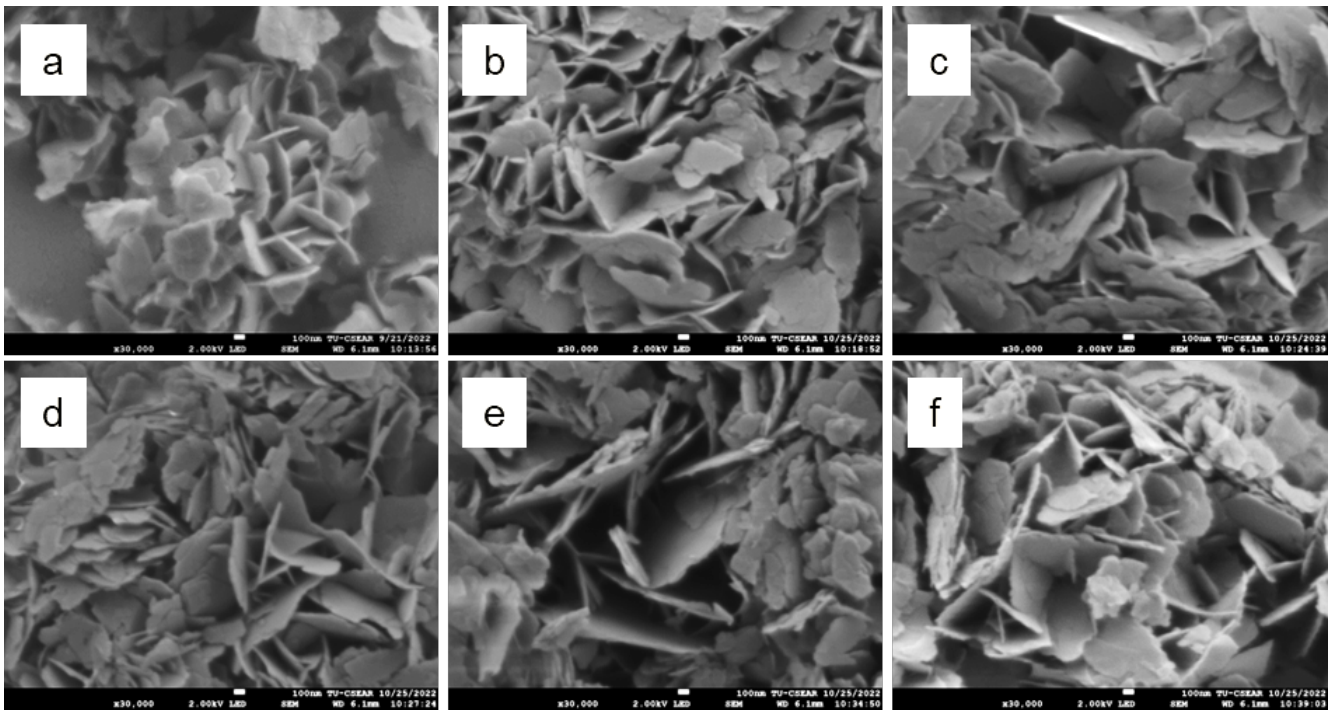

Figure 3. SEM microstructure of $Ni(OH)_2$ as a precursor source modified by electron beam irradiation technique (a) Ni(OH)2 (b) $Ni(OH_2)$ with 50 KGy of irradiation (c) $Ni(OH_2)$ with 100 KGy of irradiation (d) $Ni(OH_2)$ with 200 KGy of irradiation (e) $Ni(OH_2)$ with 300 KGy of irradiation (f) $Ni(OH_2)$ with 500 KGy of irradiation.

Figure 4 reports the size distribution of as-synthesized $Ni(OH)_2$ as a precursor source modified by electron beam irradiation technique. This technique can be used to confirm that the size of particle is in nano-scale region. The size of particle is reported as a statistical average of 220 nm. The standard deviation is also reported to be 80 nm. The size of particle was similar to previous report of Prabhu *et al.* [30]. It is in agreement with SEM analysis as reported in Figure 3.

Table 2 reports the N_2 adsorption and desorption isotherm of $Ni(OH)_2$ as a precursor source modified by electron beam irradiation technique. It is remarkable to note that specific surface area and porosity are dependent on the reactivity of the precursor source, as cited by Liu *et al.* [31]. The specific surface area is reduced when electron beam irradiation technique is employed. The role of this technique may modify the surface of particle. The range of specific surface area is dropped from 250 $m^2 \cdot g^{-1}$ to 150 $m^2 \cdot g^{-1}$. However, no significant change of pore size and pore volume are therefore observed. The data are typically presented in the region of 8 nm to 15 nm and 0.2 $cm^3 \cdot g^{-1}$ to 0.6 $cm^3 \cdot g^{-1}$, respectively. The data of specific surface area, pore size and pore volume allows us to investigate for the possibility of dye adsorption onto the surface of particle, as suggested by Saghir *et al.* [32].

Figure 5 exhibits the point of zero charge (PZC) of $Ni(OH)_2$ as a precursor source modified by electron beam irradiation technique. This strategy allows us to investigate the electrical charge onto surface of particle, as suggested by Ravichandran *et al.* [33]. It is important to note that pH significantly offers a strong effect for electrostatic interaction between the dye molecule and surface of photocatalyst [34]. The range of pH between 4 to 12 is therefore investigated.

Figure 6 presents the absorption spectra of methyl orange solution. The various conditions of electron beam irradiation onto $Ni(OH)_2$ as a precursor source are employed as a photocatalyst. All of curves are typically illustrated in the similar feature, suggesting that effect of electron beam irradiation dose do not provide the effect to the surface of photocatalyst. It is recorded that the concentration of methyl orange is reduced with respect to investigation time. It is largely dropped within 1 h. The role of photocatalyst can degrade the methyl orange molecules. When a catalyst is exposed to light with photon energy, electron is activated to the conduction band from the valence band. The free electron and hole are generated. These free ions react with O_2 and H_2O in order to form superoxide anion (O_2^-), hydroxyl (OH^-) and H_2O_2 radicals. Methyl orange molecule can be therefore decomposed into CO_2 and H_2O [35,36].

Figure 7 exhibits the dye adsorption capacity and efficiency of dye adsorption of $Ni(OH)_2$ as a precursor source modified by electron beam irradiation technique. It is observed for adsorption capacity over methyl orange molecule. The adsorption capacity is observed within (1-3) $\times 10^{-5}$ M. No significant change of adsorption based on concentration is observed. The adsorption capacity and efficiency are still existed in the similar level. Furthermore, with the variation of electron beam irradiation dose, the data are still presented in the identical form. The various doses cannot significantly offer the change for particle surface.

Table 2. BET analysis of $Ni(OH)_2$ as a precursor source modified by electron beam irradiation technique.

Sample	Pore size (nm)	Pore volume ($cm^3 \cdot g^{-1}$)	Specific surface area ($m^2 \cdot g^{-1}$)
0 kGy	8.3702	0.5378	248
50 kGy	14.8380	0.6070	161
100 kGy	12.4817	0.2423	182
200 kGy	10.0283	0.2109	192
300 kGy	13.4378	0.2814	197
500 kGy	10.5330	0.2540	141

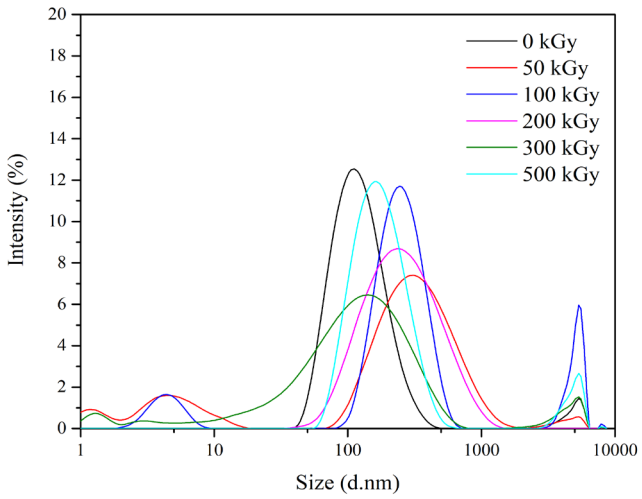

Figure 4. Size distribution analysis by dynamic light scattering of $Ni(OH)_2$ as a precursor source modified by electron beam irradiation technique.

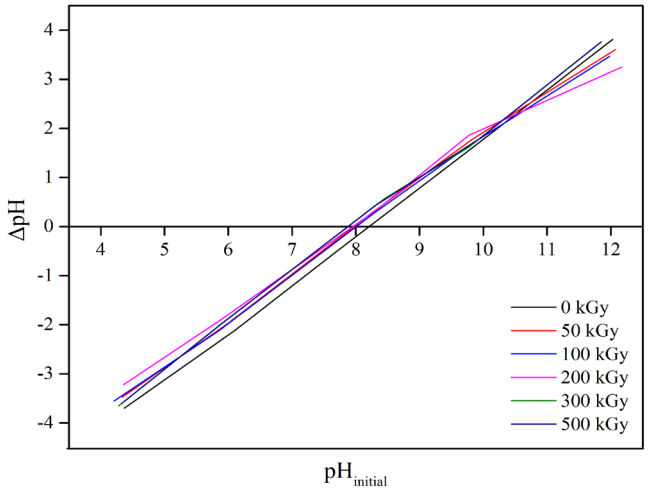

Figure 5. Point of zero charge (PZC) of $Ni(OH)_2$ as a precursor source modified by electron beam irradiation technique.

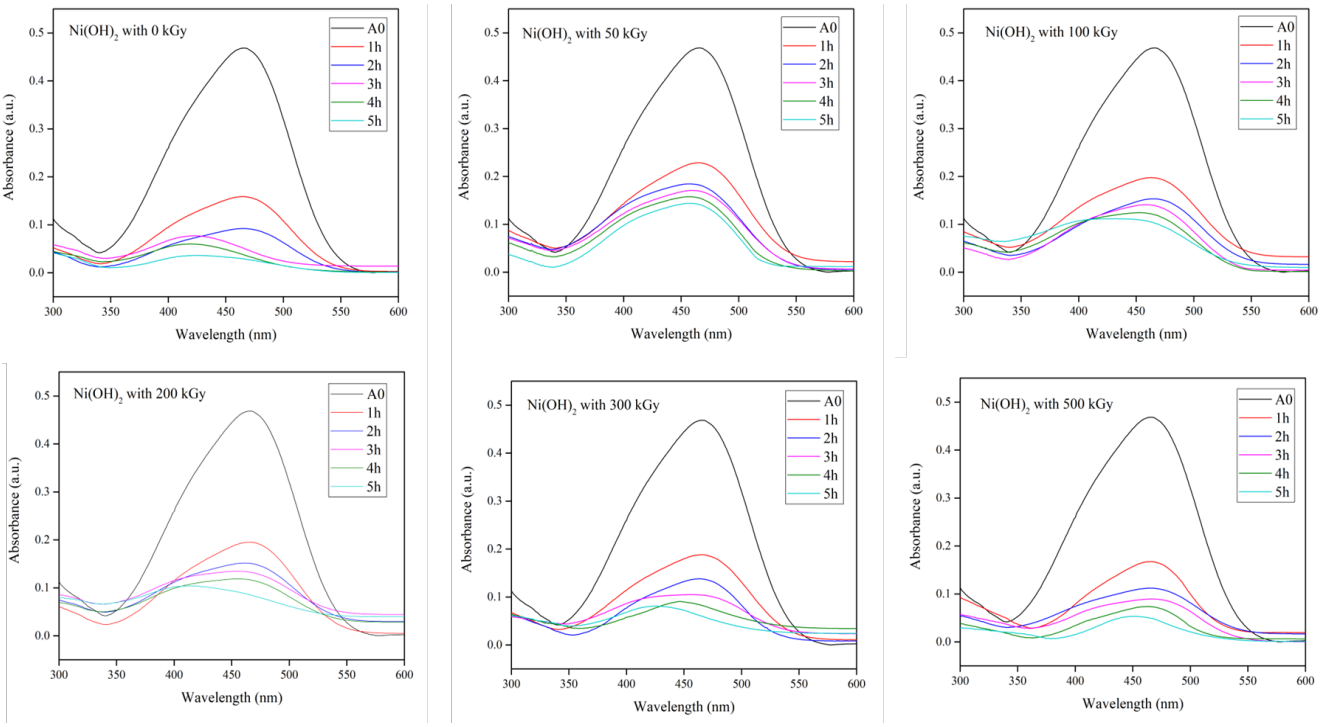

Figure 6. UV-Vis spectra of methyl orange absorption of $Ni(OH)_2$ as a precursor source modified by electron beam irradiation technique.

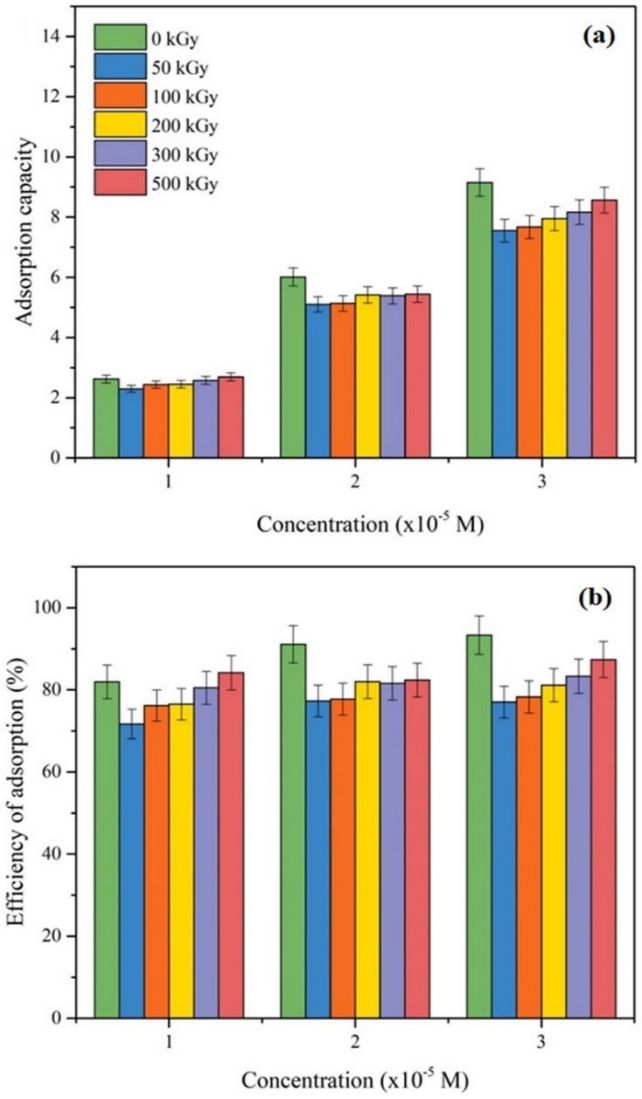

Figure 7. (a) Dye adsorption capacity (b) Efficiency of dye adsorption of $Ni(OH)_2$ as a precursor source modified by electron beam irradiation technique.

4. Conclusion

$Ni(OH)_2$ particle is successfully synthesized by self-assembly technique. This technique allows us to synthesize the nanoparticle based on thermodynamic equilibrium. No significant change of functional group and crystal phase of particles are observed by FTIR and XRD analysis. Electron beam irradiation technique interacts the surface of particle. However, due to the insufficient energy, it can be significantly changed the surface properties of as-synthesized particle. The percent of crystallinity is dropped from 86.56% to 82.85%. The crystal size is slightly reduced due to interaction of electron beam. The uniform distribution is observed by DLS analysis. Smaller size may agglomerate to form a larger size. The specific surface area, pore size and pore volume are decreased. The morphology of particle is uniformly presented as a plate-like structure. The electrical charge is positive. It can be remarkably noted that as-synthesized particle exhibits the outstanding properties for negative charge of dye adsorption. It illustrates the excellent properties for methyl orange adsorption and photocatalyst for dye degradation.

Acknowledgment

This work is mainly supported by the funding under TINT to University project (2566), Thailand Institute of Nuclear Technology (TINT), Thailand. One (S.U.) of the authors would like to acknowledge the support from Thammasat University Research Unit in Textile and Polymer Chemistry. Last, but not least, S.U. would like to acknowledge the fund by Hub of Talent: Sustainable Materials for Circular Economy, National Research Council of Thailand (NRCT).

References

[1] Y. Liao, J. Wang, M. Feng, S. Zhu, M. Chen, and F. Wang, "Self healing behavior of enamel incorporated with nickel particles of various sizes during high temperature oxidation process," *Corrosion Communications*, vol. 8, pp. 49-57, 2022.

[2] J. Li, R. Liu, Q. Song, Z. Gao, H. Huang, Q. Zhang, X. Shi , S. Bai, and L. Chen, "Enhanced thermal stability and oxidation resistance in La_3-xTe_4 by compositing metallic nickel particles," *Acta Materialia*, vol. 224, p. 117526, 2022.

[3] I. Fatimah, P. W. Citradewi, G. Purwiandono, H. Hidayat, and S. Sagadevan, "Nickel oxide decorated reduced graphene oxide synthesized using single bioreductor of Pometia pinnata leaves extract as photocatalyst in tetracycline photooxidation and anti-bacterial agent," *Inorganic Chemistry Communications*, vol. 148, p. 110287, 2023.

[4] T. R. Kuo, I. Fitriannisa, R. J. Chung, K. H. Lin, S. Yougbaré, L. Y. Lin, and Y. F. Wu, "Facile synthesis of copper cobalt sulfide and nickel hydroxide tube-like composites as battery-type active material of energy storage devices," *journal of Energy storage*, vol. 65, p. 107330, 2023.

[5] L. Zhao, F. Meng, and W. Zhang, "Rational design and synthesis of nickel-cobalt-manganese trimetallic hydroxides with microflower like for high-performance asymmetric super-capacitors," *Materials Chemistry and Physics*, vol. 290, p. 126641, 2022.

[6] S. D. Dhas, P. S. Maldar, M. D. Patil, M. R. Waikar, R. G. Sonkawade, and A. V. Moholkar, "Sol-gel synthesized nickel oxide nanostructures on nickel foam and nickel mesh for a targeted energy storage application," *Journal of Energy Storage*, vol. 47, pp. 103658, 2022.

[7] V. Karol, C. Prakash, and A. Sharma, "Impact of magnesium content on various properties of $Ba_{0.95}$-x$Sr_{0.05}Mg_xTiO_3$ ceramic system synthesized by solid state reaction route," *Materials Chemistry and Physics*, vol. 271, p. 124905, 2021.

[8] L. Durai, A. Gopalakrishnan, and S. Badhulika, "One-pot hydro-thermal synthesis of NiCoZn a ternary mixed metal oxide nano-rod based electrochemical sensor for trace level recognition of dopamine in biofluids," *Materials Letters*, vol. 298, p. 130044, 2021.

[9] P. Noppakuadrittidej, K. Tonsomboon, and S. Ummartyotin, "Importance of solvent singularity on the formation of highly uniform hexagonal close packed (HCP) colloidal monolayers during spin coating," *Colloid and Interface Science Communications*, vol. 30, p. 100177, 2019.

[10] N. Phutanon, P. Pisitsak, H. Manuspiya, and S. Ummartyotin, "Synthesis of three-dimensional hierarchical CuO flower-like architecture and its photocatalytic activity for rhodamine b degradation," *Journal of Science: Advanced Materials and Devices*, vol. 3, no. 3, pp. 310-316, 2018.

[11] S. Aejitha, G. Dhanraj, T. Govindaraj, N. Senthilkumar, F. Maiz, M. Shkir, W. K. Kim, V. R. M. Reddy, and D. H. Kim, "Effect of La-doping on NiO photocatalyst for enhancing photocatalytic degradation performance under visible light irradiation: DFT calculations and degradation mechanism," *Inorganic Chemistry Communications*, vol. 156, p. 111172, 2023.

[12] S. A. H. Moradi, N. Ghobadi, and S. M. Tabatabaeinejad, "Facile and rapid preparations of progressive ZnO/NiO/rGO nanophotocatalyst and investigaton its mechanism and reaction kinetics while decomposition of pharmaceuticals pollutant," *Surfaces and Interfaces,* vol. 39, p. 102939, 2023.

[13] I. Ahmad, Y. Zou, J.Yan, Y. Liu, S. Shukrullah, M. Y. Naz, H. Hussain, W. Q. Khan, and N. R. Khalid, "Semiconductor photocatalysts: A critical review highlighting the various strategies to boost the photocatalytic performances for diverse applications," *Advances in Colloid and Interface Science*, vol. 311, p. 102830, 2023.

[14] W.-Q. Li, and C.-Y. Mu, "Charging effects of SiO_2 thin film on Si substrate irradiated by penetrating electron beam," *Micron*, vol. 140, p. 102961, 2021.

[15] S. Y. Sokovnin, M. E. Balezin, and V. G. Ilves, "Effect of electron beam irradiation on the magnetic, thermal and luminescence properties of various oxide metal nanopowders," *Materials Chemistry and Physics*, vol. 215 , pp. 127-136, 2018.

[16] J. Kugai, T. Moriya, S. Seino, T. Nakagawa, Y. Ohkubo, K. Ueno, H. Nitani, and T. A. Yamamoto, "Structure of bicomponent metal-oxide composites synthesized by electron beam irradiation method," *Journal of Alloys and Compounds*, vol. 577, pp. 125-130, 2013.

[17] N. Phutanon, K. Motina, Y. H. Chang, and S. Ummartyotin, "Development of CuO particles onto bacterial cellulose sheets by forced hydrolysis: A synergistic approach for generating sheets with photocatalytic and antibiofouling properties," *International Journal of Biological Macromolecules*, vol. 136, pp. 1142-1152, 2019.

[18] J. Kim, J. Yun, X. Wen, A. Soufiani, C. Lau, B. Wilkinson, J. Seidel, M. Green, S. Huang, and A. Ho-baillie, "Nucleation and growth control of Hc(Nh2)2pbi3 for planar perovskite solar cell," *Journal of Physical Chemistry C*, vol. 120 , p. 11262, 2016.

[19] D. Musino, C. Rivard, G. Landrot, B. Novales, T. Rabilloud, and I. Capron, "Hydroxyl groups on cellulose nanocrystal surfaces form nucleation points for silver nanoparticles of varying shapes and sizes," *Journal of Colloid and Interface Science*, vol. 584, pp. 360-371, 2021.

[20] A. R. Lokanathan, K. M. A. Uddin, O. J. Rojas, and J. Laine, "Cellulose nanocrystal-mediated synthesis of silver nano-particles: Role of sulfate groups in nucleation phenomena," *Biomacromolecules*, vol. 15, no. 1 , pp. 373-379, 2014.

[21] P. Raveendran, J. Fu, and S. L Wallen, "Completely "Green" synthesis and stabilization of metal nanoparticles," *Journal of the American Chemical Society*, vol. 125, no. 46, pp. 13940-13941, 2003.

[22] P. Lv, X. Sun, J. Cai, C. Zhang, X. Liu, and Q. Guan, "Microstructure and high temperature oxidation resistance of nickel based alloy GH4169 irradiated by high current pulsed electron beam," *Surface and Coatings Technology*, vol. 309, pp. 401-409, 2017.

[23] K. Akhtar, S. B. Khan, E. M. Bakhsh, and A. M. Asiri, "A nanocomposite of nickel oxide-tin oxide and carboxymethyl-cellulose coated cotton fibres for catalytic reduction of water pollutants," *Journal of Molecular Liquids*, vol. 375, p. 121275, 2023.

[24] C. Meid, A. Dennstedt, M. Ramsperger, J. Pistor, B. Ruttert, I. Lopez-Galilea, W. Theisen, C. Körner, and M. Bartsch, "Effect of heat treatment on the high temperature fatigue life of single crystalline nickel base superalloy additively manufactured by means of selective electron beam melting," *Scripta Materialia*, vol. 168, pp. 124-128, 2019.

[25] D. Wang, R. Xu, X. Wang, and Y. Li, "NiO nanorings and their unexpected catalytic property for CO oxidation," *Nanotechnology*, vol. 17, no. 4, pp. 979-983, 2006.

[26] P. Oliva, J. Leonardi, J. F. Laurent, C. Delmas, J. J. Braconnier, M. Figlarz, F. Fievet, and A. de Guibert, "Review of the structure and the electrochemistry of nickel hydroxides and oxy-hydroxides," *Journal of Power Sources*, vol. 8, no. 2, pp. 229-255, 1982.

[27] C. Delmas, and C. Tessier, "Stacking faults in the structure of nickel hydroxide: a rationale of its high electrochemical activity," *Journal of Materials Chemistry*, vol. 7, no. 8, pp. 1439-1443, 1997.

[28] A. A. S. Gonçalves, and M. Jaroniec, "Evaporation-induced self-assembly synthesis of nanostructured alumina-based mixed metal oxides with tailored porosity," *Journal of Colloid and Interface Science*, vol. 537, pp. 725-735, 2019.

[29] X. Li, Y. Chen, C. Xiao, Y. Hu, H. Liu, Y. Chen, and J. Cheng, "Manipulating the morphology of self-assembly broccoli-like cobalt nickel spinel for enhancing the peroxydisulfate activation towards highly-effective ciprofloxacin degradation: Radical and non-radical pathways, mechanism and toxicity evaluation," *Applied Surface Science*, vol. 617, p. 156593, 2023.

[30] S. Prabhu, T. D. Thangadurai, P. V. Bharathy, and P. Kalugasalam, "Synthesis and characterization of nickel oxide nanoparticles using Clitoria ternatea flower extract: Photocatalytic dye degradation under sunlight and antibacterial activity applications," *Results in Chemistry*, vol. 4, p. 100285, 2022.

[31] G. Liu, L. Qiu, H. Deng, J. Wang, L. Yao, and L. Deng, "Ultrahigh surface area carbon nanosheets derived from lotus leaf with super capacities for capacitive deionization and dye adsorption," *Applied Surface Science*, vol. 524, p. 146485, 2020.

[32] S. Saghir, C. Pu, E. Fu, Y. Wang, and Z. Xiao, "Synthesis of high surface area porous biochar obtained from pistachio shells for the efficient adsorption of organic dyes from polluted water," *Surfaces and Interfaces*, vol. 34, p. 102357, 2022.

[33] K. Ravichandran, N. S. Jyothi, K. Thirumurugan, S. Suvathi, N. Chidhambaram, R. Uma, and B. Sundaresan, "Influence of $Mo^{+}F$ incorporation and point of zero charge on the dye degradation efficacy of ZnO thin films," *Chemical Physics*, vol. 564, p. 111714, 2023.

[34] H. A. Kiwaan, F. Sh. Mohamed, N. A. El-Ghamaz, N. M. Beshry, and A. A. El-Bindary, "Experimental and electrical studies of Na-X zeolite for the adsorption of different dyes," *Journal of Molecular Liquids*, vol. 332, p. 115877, 2021.

[35] V. S. Sonam, S. Chetana, A. Rohini, and R. G. Parag, "Synthesis of ultrasound assisted nanostuctured photocatalyst (NiO supported over CeO_2) and its application for photocatalytic as well as sonocatalytic dye degradation," *Catalysis Today*, vol. 300, pp. 50-57, 2018.

[36] M. Ismael, "Facile synthesis of NiO-loaded g-C_3N_4 heterojunction photocatalyst for efficient photocatalytic degradation of 4-nitrophenol under visible light irradiation," *Journal of Photochemistry and Photobiology A: Chemistry*, vol. 439, p. 114576, 2023.